JACS
JOURNAL OF THE AMERICAN CHEMICAL SOCIETY
Article
pubs.acs.org/JACS

Rifamycin Biosynthetic Congeners: Isolation and Total Synthesis of Rifsaliniketal and Total Synthesis of Salinisporamycin and Saliniketals A and B

Yu Feng,[†] Jun Liu,[†] Yazmin P. Carrasco,[†] John B. MacMillan,*[,†] and Jef K. De Brabander*[,†,‡]

[†]Department of Biochemistry and [‡]Harold C. Simmons Comprehensive Cancer Center, The University of Texas Southwestern Medical Center at Dallas, 5323 Harry Hines Boulevard, Dallas, Texas 75390-9038, United States

Supporting Information

ABSTRACT: We describe the isolation, structure elucidation, and total synthesis of the novel marine natural product rifsaliniketal and the total synthesis of the structurally related variants salinisporamycin and saliniketals A and B. Rifsaliniketal was previously proposed, but not observed, as a diverted metabolite from a biosynthetic precursor to rifamycin S. Decarboxylation of rifamycin provides salinisporamycin, which upon truncation with loss of the naphthoquinone ring leads to saliniketals. Our synthetic strategy hinged upon a Pt(II)-catalyzed cycloisomerization of an alkynediol to set the dioxabicyclo[3.2.1]octane ring system and a fragmentation of an intermediate dihydropyranone to forge a stereochemically defined (*E*,*Z*)-dienamide unit. Multiple routes were explored to assemble fragments with high stereocontrol, an exercise that provided additional insights into acyclic stereocontrol during stereochemically complex fragment-assembly processes. The resulting 11−14 step synthesis of saliniketals then enabled us to explore strategies for the synthesis and coupling of highly substituted naphthoquinones or the corresponding naphthalene fragments. Whereas direct coupling with naphthoquinone fragments proved unsuccessful, both amidation and C−N bond formation tactics with the more electron-rich naphthalene congeners provided an efficient means to complete the first total synthesis of rifsaliniketal and salinisporamycin.

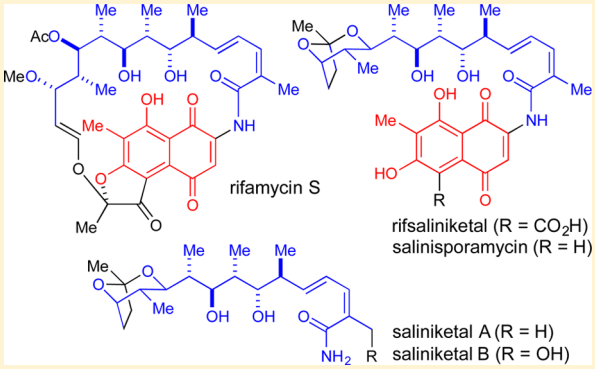

INTRODUCTION

Since the discovery of the antimalarial activity of quinine, isolated from the bark of the cinchona tree, natural products have played a fundamental role as the starting point for the discovery of drugs to combat infection, inflammation, and cancer in humans.[1] Over the past 10 years or so, marine-derived microorganisms, more specifically actinomycetes, have provided a new source of natural products. The genus *Salinispora* in particular has been a prolific producer of secondary metabolites. Currently, three species that belong to this genus have been identified: *Salinispora tropica*, *Salinispora arenicola*, and *Salinispora pacifica*.[2] The potent proteasome inhibitor salinosporamide A represents the first natural product isolated from the obligate marine bacteria *S. tropica*,[3] which is currently in clinical trials for the treatment of cancer. In 2007 the genome of *S. tropica* was sequenced to provide insight into its biosynthetic potential. It was shown that a large percentage of its genome is devoted to the assembly of natural products,[4] suggesting that there is still a large chemical diversity to explore within this genus. In this article, we document our studies of novel metabolites with a common rifamycin biosynthetic origin isolated from the marine actinomycete *S. arenicola*.

In 2007, Fenical and co-workers isolated saliniketals A (**1a**) and B (**1b**) (Chart 1) from *S. arenicola*.[5] These metabolites were isolated on the basis of their ability to prevent phorbol ester-mediated induction of ornithine decarboxylase (ODC),

Chart 1. Structures of Saliniketals A (1a) and B (1b), Salinisporamycin (2), and Rifamycin S (3)

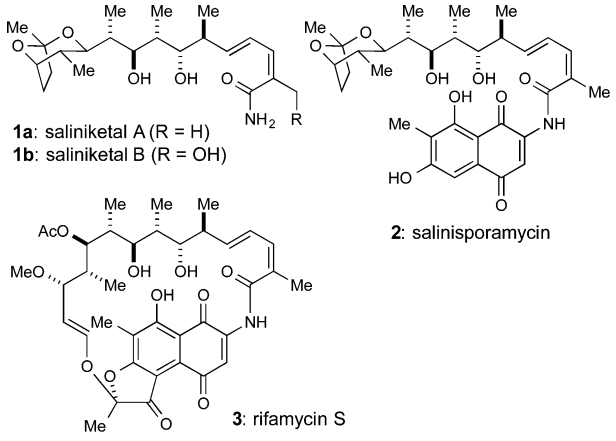

Received: March 29, 2016
Published: May 27, 2016

DOI: 10.1021/jacs.6b03248
J. Am. Chem. Soc. 2016, 138, 7130−7142

Scheme 1. Biosynthetic Relationship between Rifamycins, Rifsaliniketal, Salinisporamycin, and Saliniketals A and B[a]

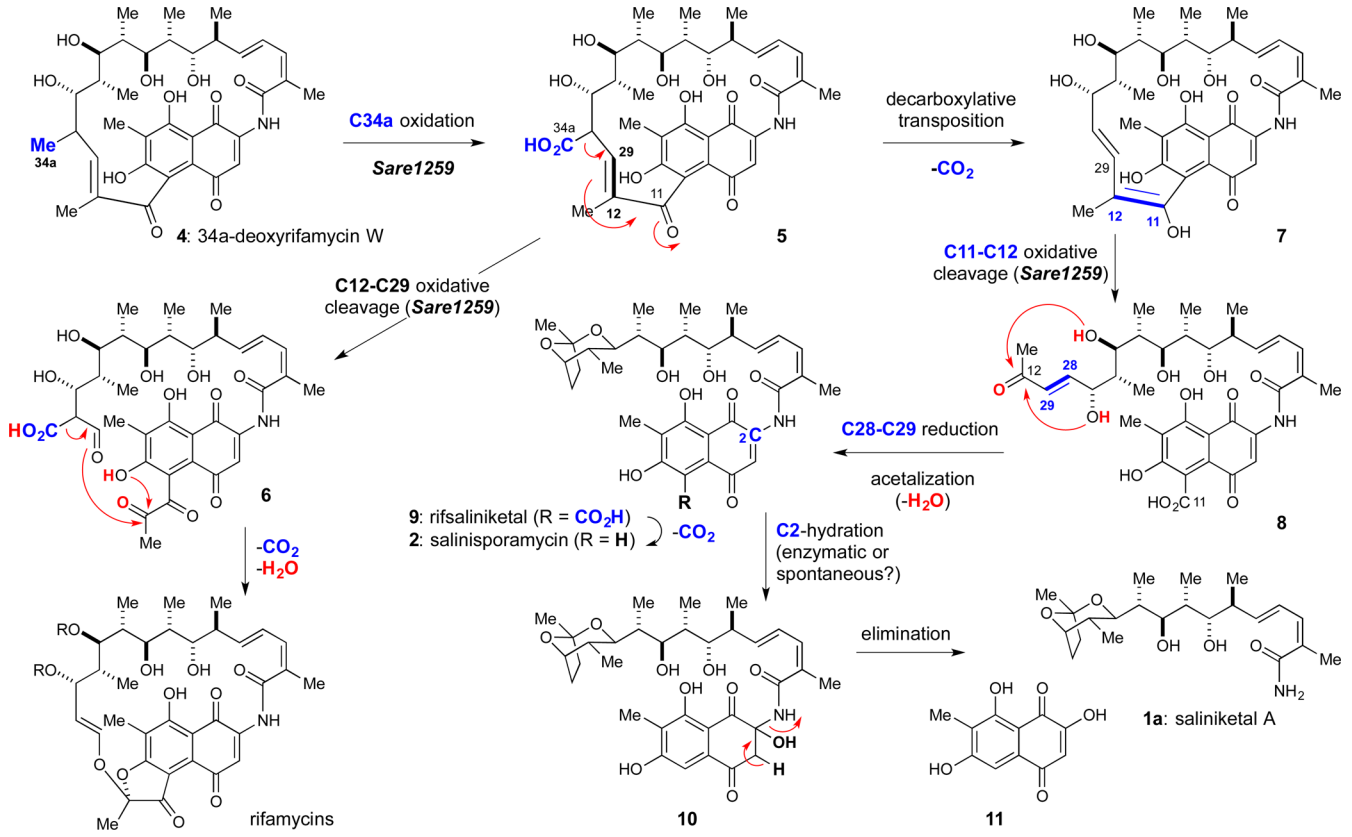

[a]Adapted from ref 14.

which is an enzyme responsible for polyamine biosynthesis.[6] Thus, by the use of T24 cells stimulated with the potent tumor promotor 12-*O*-tetradecanoylphorbol-13-acetate (TPA), saliniketals A and B were shown to inhibit TPA-induced induction of ODC with IC_{50} values of 1.95 and 7.83 μg/mL, respectively. Amino acid-derived polyamines are important for developmental processes in mice.[7] In addition, ODC is a direct target of the *MYC* oncogene, and it has been shown to be overexpressed in different tumor cells.[8] Because of their inhibitory properties against ODC induction, saliniketals may be useful as chemopreventive agents.[6,9] To date, one formal and two total syntheses of saliniketals have been disclosed, including ours.[10,11] Later, in 2009, the Matsuda group isolated a metabolite from a culture of the same species from which saliniketals were isolated (*S. arenicola*) on the basis of its ability to inhibit the growth of A549 human lung adenocarcinoma cells (IC_{50} value of 3 μg/mL).[12] Moreover, this metabolite was found to have significant activity against the bacterial strains *Staphylococcus aureus* IFO 12732 and *Bacillus subtilis* IFO 3134 with MIC values of 0.46 and 4.1 μg/mL, respectively. This compound, which they named salinisporamycin (**2**), is in essence the dihydroxynaphthoquinone amide of saliniketal A, which inter alia co-occurred in the fermentation broth. In spite of the unique 1,4-dimethyl-2,8-dioxabicyclo[3.2.1]octane ring system, salinisporamycin and saliniketals structurally appear as acyclic truncated variants of the rifamycin *ansa*-macrolide family of compounds, suggesting that they might share common biosynthetic origins. Indeed, rifamycin S (**3**), a metabolite previously observed exclusively in terrestrial soil actinobacteria (*Amycolatopsis mediterranei*), was coisolated with salinisporamycin.[12] Previously, around 2006, the groups of Fenical in California and Fuerst in Australia independently demonstrated the widespread production of rifamycins in marine *Salinispora* species.[13]

Finally, elegant studies documented by Moore and coworkers provided the first solid evidence that saliniketals and salinisporamycin are diverted products of rifamycin biosynthesis.[14] Using PCR-directed mutagenesis, chemical complementation studies, and isotope feeding experiments, they formulated a biosynthetic pathway wherein saliniketal production diverges from rifamycin production at the stage of 34a-deoxyrifamycin W (**4**) (Scheme 1). An *S. arenicola*-specific cytochrome P450 (CYP) encoded by the biosynthetic gene *sare1259* doubly oxidizes C34a to form carboxylic acid **5**, temporally regulated decarboxylation of which specifies saliniketal or rifamycin synthesis. In accordance with the proposed biosynthesis of terrestrial rifamycin, C12/C29 double-bond cleavage in intermediate **5** to form ketone aldehyde **6** prior to decarboxylation (by a CYP encoded by *sare1259* in marine *S. arenicola* or *rif-orf5* in terrestrial *A. mediterranei*) leads to rifamycin via a decarboxylative ketalization. When decarboxylation occurs prior to oxidative double-bond cleavage, the resulting C11/C12 enol **7** is then subsequently cleaved to form enone **8** upon action of the *sare1259* gene product. Subsequent C28/C29 olefin reduction followed by formation of the dioxabicyclo[3.2.1]octane ring system then provides putative intermediate **9** (which we shall term rifsaliniketal) that upon decarboxylation yields salinisporamycin (**2**), the metabolite isolated from *S. arenicola* by Matsuda and co-workers. Moore and co-workers were not able

DOI: 10.1021/jacs.6b03248
J. Am. Chem. Soc. 2016, 138, 7130−7142

to identify a *rif* pathway gene in *S. arenicola* associated with the putative conversion of **2** to saliniketal A (**1a**), suggesting that an enzyme outside the *rif* gene cluster might be responsible. Alternatively, one can envision a nonenzymatic naphthoquinone hydration (at C2 to yield **10**) followed by amide (saliniketal) elimination.

The above demonstrates the biosynthetic potential of marine microorganisms to enzymatically tailor rifamycin biosynthetic pathway intermediates for the generation of marine-specific metabolites.[14] In view of their biological activity, biosynthetic relationship to rifamycin, and novel structural features, we initiated a synthetic program directed toward saliniketals and salinisporamycin. In addition to our initial disclosure, only one total synthesis and one formal synthesis of saliniketals have been published.[10,11] No total synthesis of salinisporamycin has been described to date. Herein we describe in detail our efforts leading to the total synthesis of saliniketals A and B and the first total synthesis of salinisporamycin. In addition, we disclose for the first time the isolation (from a novel strain of *S. arenicola*), full characterization, and total synthesis of rifsaliniketal. Our studies thus lend credence to the intermediacy of this previously proposed but heretofore uncharacterized biosynthetic intermediate en route to saliniketals and salinisporamycin.[14]

RESULTS AND DISCUSSION

Isolation and Characterization of Rifsaliniketal, the Proposed Biosynthetic Precursor to Salinisporamycin and Saliniketals. During our evaluation of natural product fractions for cytotoxicity toward a panel of cancer cell lines, we identified a fraction from *S. arenicola* with potent cytotoxicity toward the human glioblastoma cell line T98G. To follow up on the activity, a 20 L scale fermentation of SNB-003 was carried out, and the secondary metabolites were extracted using XAD-7 resin. Following solvent/solvent partitioning and reversed-phase column chromatography, the fraction with activity against T98G was further purified by C18 HPLC to yield an active compound and an inactive compound. The active compound was determined to be staurosporine, whereas the inactive molecule displayed NMR signals similar to those of salinisporamycin. Further characterization led to the assignment of this compound as rifsaliniketal (**9**), validating the Moore biosynthetic proposal (Scheme 1).

Rifsaliniketal was isolated as a yellow powder with a molecular formula established as $C_{34}H_{43}NO_{11}$ based on the molecular ion peak at 642.2901 $[M + H]^+$, with 14 degrees of unsaturation calculated. On the basis of correlation spectroscopy (COSY) correlations, we were able to build the polyketide side chain of **9** and demonstrate that it is identical to that found in **1a** (Figure 1). Briefly, the C13−C18 fragment was established by COSY correlations of H15/H16, H16/H17, and H17/H18 along with key heteronuclear multiple bond correlation (HMBC) correlations from CH_3-29 (δ_H 2.08) to C13 (δ_C 169.7), C14 (δ_C 129.3), and C15 (δ_C 138.0). The C16−C17 double bond was assigned the *E* configuration on the basis of the H16/H17 proton−proton coupling constant of 15.2 Hz. COSY correlations of H18/H19 and H30, H19/H20, H20/H21 and H31, H21/H22, and H22/H23 and H32 established the C18−C23 fragment. HMBC correlations from H27 (δ_H 1.78−1.83) to C26 (δ_C 24.6), from H25 (δ_H 4.22) to C28 (δ_C 106.2), and from CH_3-33 (δ_H 1.39) to a quaternary carbon at δ_C 106.2 indicative of a ketal functionality and to C27 (δ_C 34.9) along with COSY correlations of H23/H24, H24/H25 and H34, and H25/H26 provide the assignment of the bicyclic ketal found in **9**. In addition, by means of a powerful technique that allows homonuclear decoupling of multiple neighboring protons simultaneously, we were able to obtain coupling constants of H18.[15] The proton on C18 is coupled to three distinct sets of protons, giving rise to a doublet of doublets of quartets. Application of multiple homonuclear decoupling to H17 and H30 caused H18 to collapse to a doublet with coupling to H19 (9.1 Hz). Additional decoupling of H19 and H30 collapsed H18 to a doublet coupled to H17 (8.0 Hz). Finally, decoupling of H17 and H19 collapsed H18 to a quartet coupled to H30 (6.9 Hz).

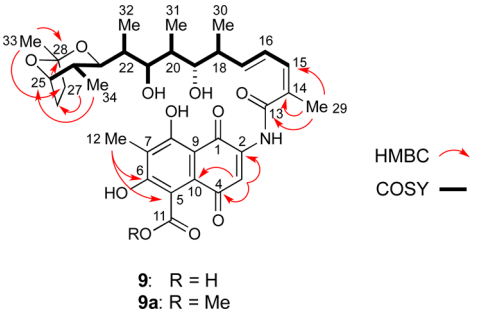

Figure 1. Selected COSY and HMBC assignments for the structural elucidation of rifsaliniketal (**9**).

A challenge in the determination of the structure of **9** was the lack of protons in the naphthoquinone ring, making it difficult to confidently assess the presence of a carboxylic acid. To circumvent this problem, we converted the carboxylic acid into its methyl ester derivative **9a** using $TMSCHN_2$. The presence of a methyl peak in the proton NMR spectrum (3.87 ppm) and a mass indicative of the methyl ester derivative ($[M + Na]^+$, *m*/*z* 678.3) together with an HMBC correlation of the resulting methyl ester to the carbonyl carbon at C11 (δ_C 172.6) validated our suspicion that in fact there was a carboxylic acid present. The remainder of the naphthoquinone core of **9** was assigned by a combination of ^{13}C chemical shift assignments and HMBC correlations from H3 (δ_H 7.66) to C2 (δ_C 141.1), C4 (δ_C 183.8), and C10 (δ_C 128.6) and from H12 (δ_H 2.16) to C6 (δ_C 162.6) and C5 (δ_C 117.5).

Overall, the NMR data for **9** were nearly identical to those of **2**.[16] All of the ansa-chain ^1H chemical shifts and coupling constants were nearly identical, while the ^{13}C chemical shifts were within 1.0 ppm. Besides the additional C11 carbonyl carbon in **9** that led to changes in the ^{13}C chemical shifts of C4 and C10, the other data for the naphthoquinone rings of **9** and **2** were very similar.

Synthesis of Saliniketals: Synthetic Strategy, Exploration of Aldol-Based Couplings, and Final Dihydropyranone Fragmentation. Structurally, saliniketals A (**1a**) and B (**1b**) are endowed with a unique 1,4-dimethyl-2,8-dioxabicyclo[3.2.1]octane ring system connected to a 2-substituted conjugated (*E*,*Z*)-dienoic carboxamide via a polypropionate-derived C5-stereopentad. Saliniketal B differs from saliniketal A by a hydroxylation at the C2-Me substituent. Whereas Paterson utilized a late-stage Stille cross-coupling approach to install the dienoic carboxamide,[10a] we opted to explore a base-mediated fragmentation (E2 elimination) of a dihydropyranone (see **12** in Scheme 2).[17] This approach imparts a higher degree of convergence by providing saliniketal's entire carbon skeleton during a late-stage aldol coupling of two enantiomerically pure C1−C7 and C8−C17

DOI: 10.1021/jacs.6b03248
J. Am. Chem. Soc. 2016, 138, 7130−7142

Scheme 2. Synthetic Strategy and Stereochemical Analysis

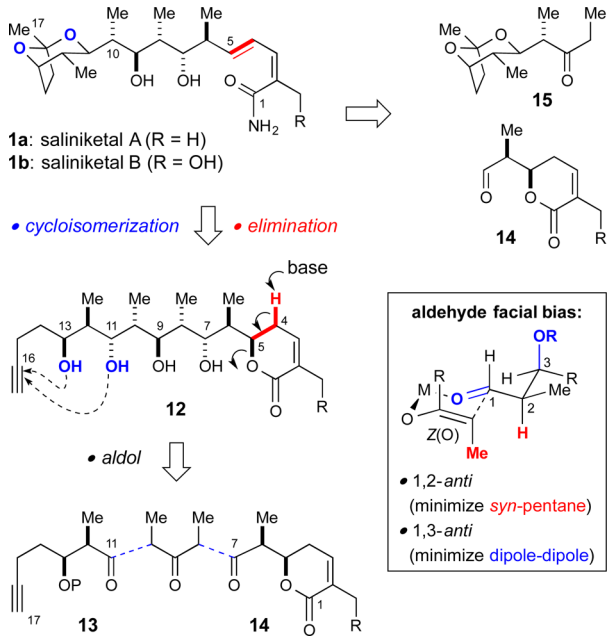

fragments (**14** and **15**, respectively). Our tactic to obtain the dioxabicyclooctane ring would rely on a Pt(II)-catalyzed cycloisomerization of a dihydroxyalkyne as previously developed by our group.[18] Paterson, on the other hand, forged this ring system using an efficient intramolecular Wacker-type cyclization of the corresponding dihydroxy-substituted terminal olefin.[10a]

Placing the above-described tactics into the proper stereochemical context—saliniketals contain eight contiguous stereocenters—is best achieved visually when focusing on structure **12** (Scheme 2). Within structure **12**, one can identify a C5–C13 stereononad with apparent C_s symmetry (symmetry plane through C9) as it relates to the nature and configuration of the branching methyl and oxygen substituents. Although the C5 stereocenter will be destroyed during our planned dihydropyranone fragmentation, one should note our judicious choice of configuration at C5 in this context. This stereochemical framework readily reveals a bidirectional aldol-based fragment coupling between 3-pentanone and aldehydes **13** and **14**.[19] According to currently accepted stereochemical models for aldol reactions of *Z*(O)-enolates via cyclic transition states, the aldehyde α-methyl and β-alkoxy substituents impart maximal reinforcing stereochemical bias when in a syn relationship by minimizing both *syn*-pentane and dipole–dipole interactions (see the box in Scheme 2).[20,21] The thus-anticipated absolute stereochemistry at the newly formed stereocenters (C7/C8 for aldol with **14** or C10/C11 for aldol with **13**) would be as shown in structure **12**. However, one cannot ignore an additional layer of complexity resulting from enolate stereochemical bias during the second of these two aldol reactions (i.e., after a C7–C8 or C10–C11 bond has been formed during the first aldol reaction), a point to which we shall return later. Suffice it for now that we ultimately settled on constructing the C10–C11 bond first (→**15**) in order to minimize protecting group manipulations (i.e., installation of the dioxabicyclooctane prior to the second aldol) and bringing in the potentially more labile dihydropyranone aldehyde **14** last during the final of these two aldol reactions.

As shown in Scheme 3, triethylsilyl-protected aldehyde **13** was readily available from commercial pent-4-ynol (**16**) in four

Scheme 3. Synthesis of Aldehyde 13 and Aldol Reaction with 3-Pentanone[a]

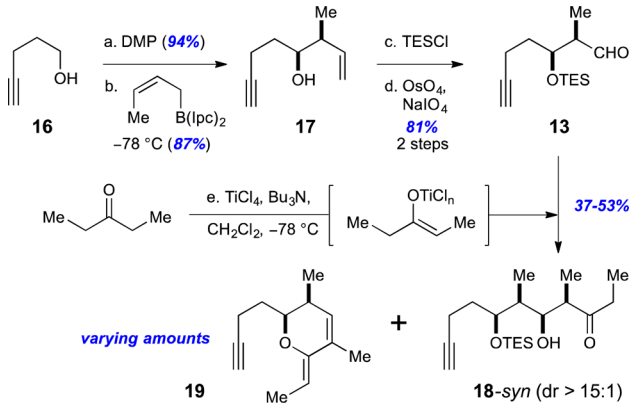

[a]Reagents and conditions: (a) Dess–Martin periodinane, CH_2Cl_2, rt, 1 h, 94%; (b) (+)-$Ipc_2B(OMe)$, ^{n}BuLi, KO^{t}Bu, *cis*-2-butene, Et_2O, −78 °C, 87%, >10:1 dr; (c) TESCl, 2,6-lutidine, CH_2Cl_2; (d) $NaIO_4$, OsO_4, 2,6-lutidine, CH_2Cl_2, 81% (two steps); (e) 3-pentanone (1 equiv), $TiCl_4$ (1.1 equiv), Bu_3N (1.2 equiv), CH_2Cl_2, −78 °C, then **13** (1.2 equiv), −78 °C, 2 h, 43–53%; or the same conditions with 3-pentanone (2 equiv), $TiCl_4$ (2.2 equiv), Bu_3N (2.4 equiv), **13** (1 equiv), 37–46%. Abbreviations: DMP, Dess–Martin periodinane; Ipc, isopinocampheyl; TES, triethylsilyl.

steps and excellent overall yields. Dess–Martin periodinane (DMP)-mediated oxidation[22] of alkynol **16** was followed by a reagent-controlled crotylation with in situ-prepared homochiral ((*Z*)-2-butenyl)diisopinocampheylborane to yield homoallylic alcohol **17**.[23] Following silylation and oxidative double-bond cleavage, the target aldehyde **13** was obtained in excellent yield. This aldehyde proved to be a frustrated partner for the ensuing aldol reaction with 3-pentanone. Reaction with lithium or boron *Z*(O)-enolates were sluggish and provided complex mixtures from which no pure identifiable products were isolated.[24] The *Z*(O)-titanium enolate proved more reactive and selective, providing a single aldol product in variable isolated yields (37–53%) but favoring the undesired (and unpredicted!) diastereomer **18**-*syn* (dr > 15:1) and varying amounts of desilylated cyclodehydrated compound **19**.[25,26] *Z*(O)-titanium enolates of achiral ethyl ketones, including 3-pentanone, have been documented to provide *anti*-Felkin products with *syn*-α-Me,β-alkoxyaldehydes (cf. **13**).[21a,b] We therefore do not understand our results in the context of current models for asymmetric induction.[27]

In an attempt to override the inherent Felkin bias of aldehyde **13**, we explored its engagement in an auxiliary-controlled Evans aldol reaction with the *Z*(O)-titanium enolate derived from (*S*)-4-benzyl-3-propionyloxazolidin-2-one (**20**) (Scheme 4).[28] Under these conditions, a 73% yield of aldol products was obtained with a dramatically improved albeit still unsatisfactory 1.2:1 ratio of the separable isomers **21**-*syn* and **21**-*anti*. Removal of the silyl protecting group followed by formation of the corresponding acetonides (**23**-*syn* and **23**-*anti*) enabled assignment of the indicated relative configuration by ^{13}C NMR analysis.[29]

Unable to override the inherent facial bias of aldehyde **13**, we took a step back and explored two alternative aldol routes starting from achiral pentynals and chiral enolates. As shown in

DOI: 10.1021/jacs.6b03248
J. Am. Chem. Soc. 2016, 138, 7130–7142

Scheme 4. Chiral-Auxiliary-Controlled Aldol Reaction with Aldehyde 13 and Stereochemical Assignment[a]

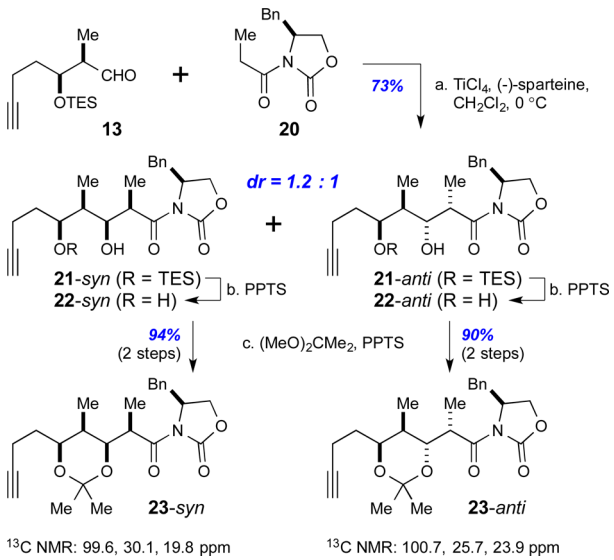

[a]Reagents and conditions: (a) **20**, $TiCl_4$, (−)-sparteine, CH_2Cl_2, 0 °C, 5 min, then **13**, 0 °C, 1 h, 73%, 1.2:1 dr; (b) PPTS, EtOH, rt; (c) PPTS (6 mol %), acetone/$(MeO)_2CMe_2$ (4:1, 0.03 M), rt, 30 min, 94% **23**-*syn* (two steps), 90% **23**-*anti* (two steps). Abbreviations: Bn, benzyl; PPTS, pyridinium *p*-toluenesulfonate.

Scheme 5A, reaction of the *Z*(O)-boron enolate derived from chiral ethyl ketone **25** with aldehyde **24** (prepared from commercial alcohol **16** via DMP oxidation in 94% yield; see Scheme 3)[22] using a protocol pioneered by Paterson and co-workers[10a] afforded the desired *anti*-dimethyl aldol product **26**

Scheme 5. Two Successful Routes to Correctly Configured Stereotetrads 27 and 22-*anti*[a]

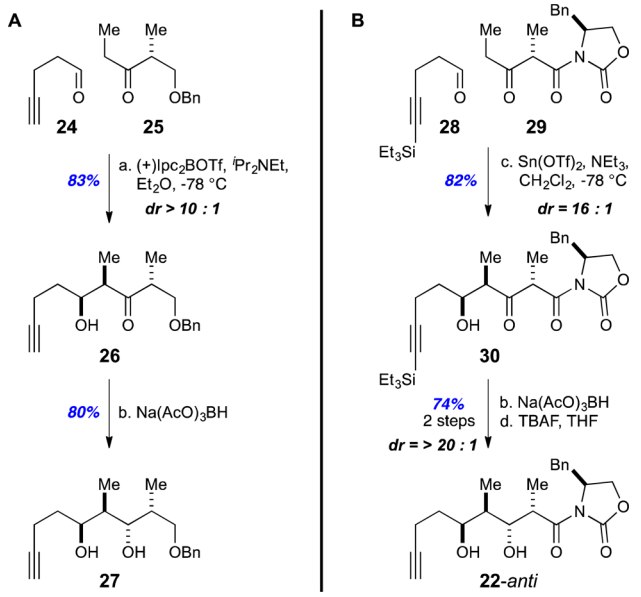

[a]Reagents and conditions: (a) (+)-Ipc_2BOTf, $^iPr_2NEt$, Et_2O, −78 °C, 83%, >10:1 dr; (b) $NaBH_4$, HOAc, 0 °C to rt; (c) **29**, $Sn(OTf)_2$, Et_3N, CH_2Cl_2, −20 °C, then −78 °C, **28**, 82%, 16:1 dr; (d) TBAF, THF, 3 min, 94%. Abbreviations: TBAF, tetrabutylammonium fluoride; Tf, trifluoromethanesulfonyl.

with high selectivity (>10:1 dr) in 83% yield. An anti-selective sodium triacetoxyborohydride reduction delivered the desired stereotetrad **27** in 80% yield.[30] Alternatively, aldol reaction of the stannyl enolate derived from known oxazolidinone **29** with aldehyde **28** (obtained from DMP oxidation of the corresponding commercially available alkynol in 92% yield)[22] provided aldol product **30** in 82% yield with >16:1 dr.[31] Anti-selective reduction with $Na(OAc)_3BH$ (>20:1 dr)[30] followed by desilylation afforded stereotetrad **22**-*anti* (74% yield over two steps).[32]

As discussed previously (Scheme 2), we planned to construct the saliniketal dioxabicyclooctane ring system by means of a Pt(II)-catalyzed cycloisomerization of a dihydroxyalkyne as previously developed by us.[18] The availability of a set of different alkynediols provided a solid basis to further investigate the scope and limitations of this methodology (Table 1). As

Table 1. Pt(II)-Catalyzed Cycloisomerization of Dihydroxyalkynes[a]

Entry	Substrate	Product (Yield)[b]
1	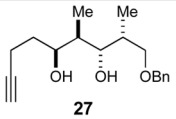 **27**	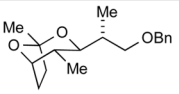 **32** (**95%**)
2	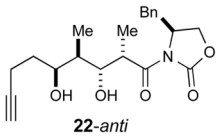 **22**-*anti*	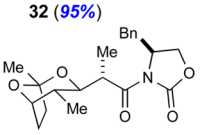 **33** (**99%**)
3	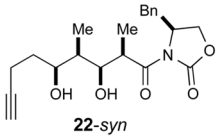 **22**-*syn*	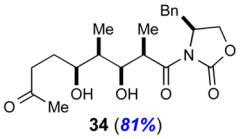 **34** (**81%**)
4	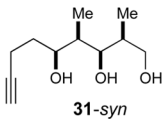 **31**-*syn*	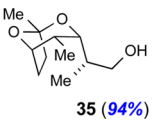 **35** (**94%**)

[a]Reaction conditions: substrate (0.1 mmol), $[PtCl_2(CH_2CH_2)]_2$ (5 mol %), THF, rt. [b]Yields of isolated purified products.

shown in entries 1 and 2, we were pleased to observe that substrates with stereochemistry reminiscent of saliniketals (**27** and **22**-*anti*) were smoothly converted to 1,4-dimethyl-2,8-dioxabicyclo[3.2.1]octanes **32** and **33**, respectively, in >95% yield upon stirring with a catalytic amount of Ziese's dimer ($[PtCl_2(CH_2CH_2)]_2$, 5 mol %) in THF at ambient temperature. Interestingly, the diastereomeric dihydroxyalkyne **22**-*syn* was recalcitrant toward cycloisomerization and instead was converted to terminal methyl ketone **34** in 81% yield via competing hydration of the alkyne (entry 3), whereas the reduced triol substrate **31**-*syn* (entry 4) did proceed to yield the diastereomeric dioxabicyclooctane **35**, but only after a substantially prolonged reaction time of 1.5 h (vs 5 min for entries 1 and 2).

The above results are perhaps most easily explained in the context of concepts formulated in Scheme 6. Upon treatment with the π acid ($[PtCl_2(CH_2CH_2)]_2$, the terminal alkyne, generically represented by structure **36**, is activated for a kinetically facile 5-exo cyclization to provide, after proton transfer, the putative oxonium intermediate **37** (Scheme 6A), which is trapped via 6-endo spiroketalization to deliver, after

DOI: 10.1021/jacs.6b03248
J. Am. Chem. Soc. 2016, 138, 7130−7142

Scheme 6. Rationalization of the Results Presented in Table 1

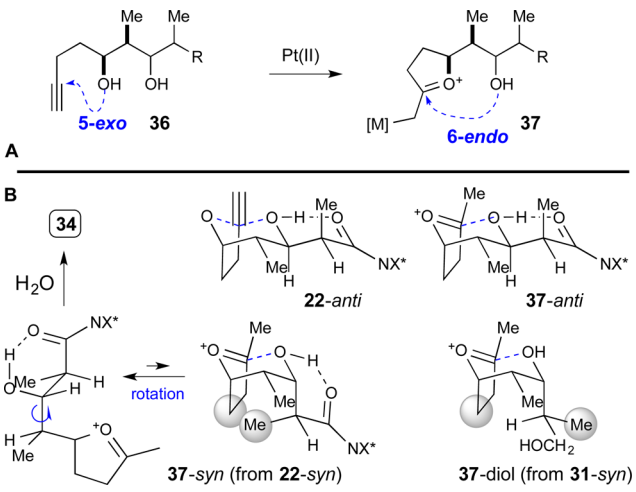

protodemetalation, the dioxabicyclo[3.2.1]octane ring system.[18] As shown in Scheme 6B, low-energy chair conformations of anti-configured substrates that avoid *syn*-pentane interactions, as exemplified by **22**-*anti* and its in situ-generated oxomium intermediate **37**-*anti*, are readily accessible and allow facile, rapid spiroketalization, as documented in Table 1, entries 1 and 2. Such low-energy conformations are not accessible for **22**-*syn* and **31**-*syn*. Although the formation of intermediate oxonium **37** occurs unimpeded, potential transition states for intramolecular addition of the second alcohol (6-endo) do appear to suffer steric consequences, as represented by **37**-*syn* and **37**-diol. Potential alternate conformations (not shown) also suffer steric penalties compared with cyclization intermediate **37**-*anti*. For intermediate **37**-*syn*, this leads to competitive hydrolysis to give ketone **34** (entry 3), whereas **37**-diol did provide bicyclic ketal **35** but at a greatly reduced rate (entry 4).

With the cycloisomerization accomplished, oxazolidinone **33** was processed to obtain ethyl ketone **15** via Weinreb amide formation and Grignard reaction with ethylmagnesium bromide (87% for two steps; Scheme 7). Alternatively, hydrogenolysis of

Scheme 7. Two Routes for the Synthesis of Ethyl Ketone 15[a]

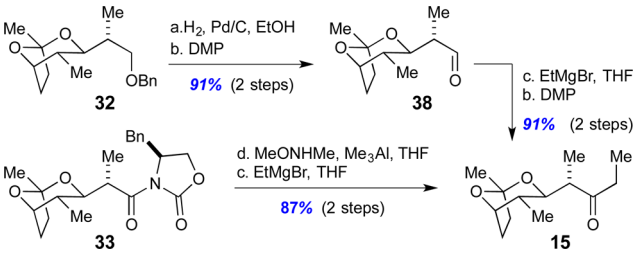

[a]Reagents and conditions: (a) H_2, Pd/C, EtOH, 2 h, rt, 96%; (b) DMP, $NaHCO_3$, CH_2Cl_2; (c) EtMgBr, THF, 0 °C, 1 h; (d) MeONHMe·HCl, $AlMe_3$, THF, 0 °C.

benzyl ether **32** provided an alcohol that was identical to the one reported by Paterson and co-workers.[10a,32] This alcohol was oxidized to aldehyde **38**, which was followed by Grignard addition (EtMgBr) and another Dess–Martin oxidation to form ketone **15**. Thus, key coupling fragment **15** was reproducibly available in eight or nine steps (longest linear sequence) from commercially available materials via two alternative and equally efficient routes (45–55% overall yield).

The synthesis of the aldehyde coupling partners **14a** and **14b** is based on the conceptually simple and practical approach depicted in Scheme 8. According to a sequence adapted from

Scheme 8. Synthesis of Coupling Fragments 14a and 14b[a]

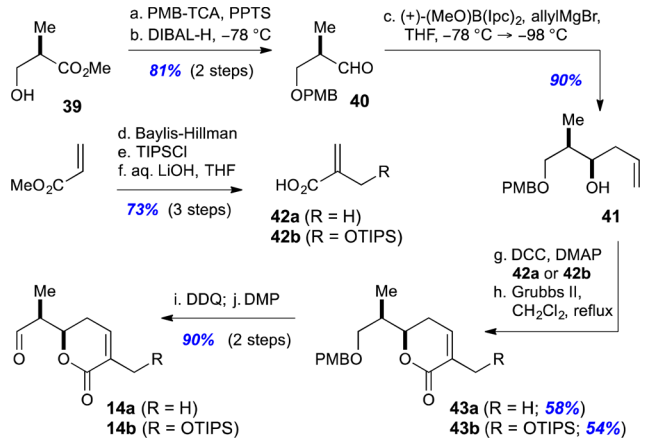

[a]Reagents and conditions: (a) 4-MeOBnOC(NH)CCl_3, PPTS, CH_2Cl_2, rt, 18 h, 87%; (b) DIBAL-H, CH_2Cl_2, −78 °C, 2 h, 93%; (c) (+)-MeOB(Ipc)$_2$, allylMgBr, 0 °C, add **40**, −98 °C, then NaOH, 30% H_2O_2, Et_2O, reflux, 90%; (d) paraformaldehyde, DABCO, dioxane/H_2O (1:1), 72 h; (e) TIPSCl, imidazole, DMAP, CH_2Cl_2, 0 °C to rt, 1 h, 79% (two steps); (f) LiOH, THF/H_2O (1:1), rt, 36 h, 92%; (g) DCC, DMAP, CH_2Cl_2, 0 °C to rt, 12 h, 90% from **42a**, 82% from **42b**; (h) Grubbs-II (10 mol %), CH_2Cl_2, reflux, 14 h, 64% **43a** (+12% recovered SM), 67% **43b** (+15% recovered SM); (i) DDQ, CH_2Cl_2/H_2O (20:1), rt, 1 h; (j) DMP, $NaHCO_3$, CH_2Cl_2, rt, 30 min, 90% **14a** or **14b** (two steps). Abbrevations: DABCO, 1,4-diazabicyclo[2.2.2]octane; DDQ, 2,3-dichloro-5,6-dicyano-1,4-benzoquinone; DCC, dicyclohexylcarbodiimide; DIBAL-H, diisobutylaluminum hydride; DMAP, 4-dimethylaminopyridine; PMB-TCA, *p*-methoxybenzyl trichloroacetimidate; TIPS, triisopropylsilyl.

Nicolaou and co-workers, protection and semireduction of Roche ester **39** was followed by a highly selective reagent-controlled Brown allylation of aldehyde **40** to provide syn homoallylic alcohol **41** in 73% overall yield for the three steps.[33,34] Esterification of this material with methacrylic acid (**42a**) or its oxygenated congener **42b** (prepared from methyl acrylate via Baylis–Hillman reaction,[35] silylation, and saponification in 73% overall yield) set the stage for a ring-closing metathesis that provided dihydropyranones **43a** and **43b**.[36] A final oxidative deprotection (DDQ, 90%) and oxidation with DMP (quantitative) delivered aldehydes **14a** and **14b** in seven steps and 35–36% overall yield from commercial starting material.

We next investigated the key aldol coupling reaction (Scheme 9). As discussed during the retrosynthetic analysis, the predicted *anti*-Felkin bias of aldehyde **14** in aldol reactions with *Z*(O)-enolates would provide the stereochemical outcome for saliniketals.[20,21] In regard to coupling partner **15**, the facial bias of chiral *α*-Me,*β*-alkoxy-substituted *Z*(O)-enolates is primarily dominated by the *α*-stereocenter and strongly influenced by the enolate counterion.[21,37,38] Whereas titanium[21a,b] and boron[37c,d] enolates provide *syn*-dimethyl aldol products (referring to the product ketone *α*- and *α*′-Me substituents) with high selectivity, the corresponding lithium enolates are generally less selective,[21a,c,37a,b] but importantly,

DOI: 10.1021/jacs.6b03248
J. Am. Chem. Soc. 2016, 138, 7130–7142

Scheme 9. Highly Selective Aldol Fragment Coupling

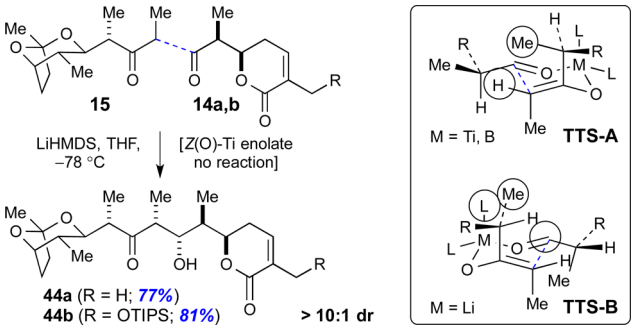

they exhibit a preference for the opposite *anti*-dimethyl aldol product. These observations are conveniently rationalized via consideration of chairlike transition states **TTS-A** and **TTS-B** (see the box in Scheme 9, in which circles indicate potentially relevant nonbonding interactions). Minimization of nonbonding interactions between the enolate chiral α-substituent and metal ligands dominate for the more compact transition states with titanium (also boron) enolates, which is best accomplished via **TTS-A**. Minimization of allylic $A^{1,3}$ strain as in **TTS-B**, on the other hand,[39] is potentially a more important contributor for reactions with lithium enolates, which proceed via a looser transition state because of the shorter Ti−O bond length versus Li−O.[40]

The above analysis predicted a fully matched situation for a titanium enolate reaction with aldehyde partners **14a** and **14b** to yield the desired aldol products **44a** and **44b** (**TTS-A**, *anti*-Felkin aldehyde face).[21b] Unfortunately, all attempts to engage titanium enolates derived from **15** proved fruitless, leading to decomposition of ketone **15** and recovery of aldehydes **14a** and **14b**. The lithium enolate of **15**, on the other hand, was predicted to provide low selectivity due to a developing *syn*-pentane interaction between the enolate and aldehyde methyl substituents, as shown in **TTS-B** (mismatch with Felkin aldehyde face).[20a,21c,41] Surprisingly, however, aldol products **44a** and **44b** were obtained in high yields and selectivity (>10:1), indicating that the reaction had proceeded via *anti*-Felkin attack of the enolate *Si* face to aldehydes **14a** and **14b**, as if it had behaved as a *Z*(O)-titanium enolate (see **TTS-A**).

This unexpected yet fortuitous outcome deserves some comment. Inspection of the four staggered (C−C bond between the α- and β-stereocenters) lithium enolate conformations **I**−**IV** depicted in Figure 2 (two each with H,H and H,Me $A^{1,3}$ enolate conformation) reveals a potential defining role for the γ-Me substituent. In the absence of this substituent (light-gray circle), conformations **I** and **IV** best minimize steric strain and dipole−dipole interactions, of which $A^{1,3}$-minimized conformation **I** is expected to engage in *Si*-face aldol reactions, as shown in **TTS-B** (Scheme 9). The γ-Me substituent, however, raises the energy of conformations **I** and **III** by virtue of a *syn*-pentane interaction with the enolate carbon (dark-gray circle), leading to the observed *Re*-face attack via conformation **IV** (see **TTS-A (Li)** in the right box). Although we cannot rule out a chelation model via inside (*Re*-face) attack on conformation **II**, which would lead to the observed stereochemical outcome, we disfavor this possibility because of the developing *syn*-pentane interactions with the ethylene bridge (**TTS-chelate**, left box) and because other lithium enolates derived from α-Me,β-alkoxy ethyl ketones but lacking this

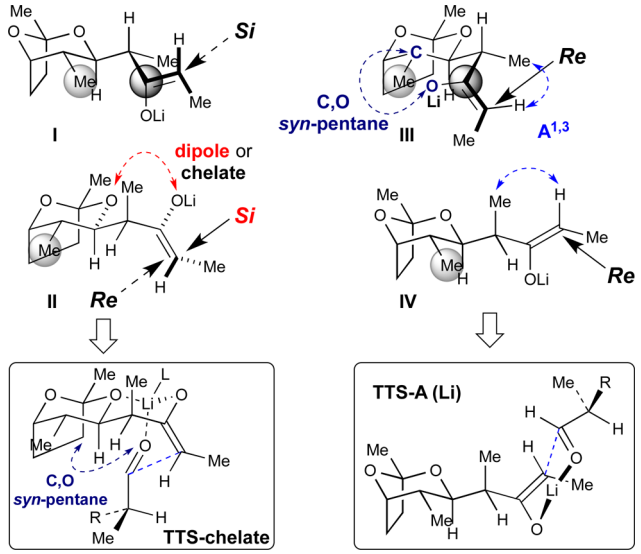

Figure 2. Conformational analysis of lithium enolates derived from ethyl ketone **15**.

additional offending *syn*-pentane interaction nevertheless provide the opposite stereochemical outcome.[42]

Having achieved a highly selective aldol coupling, we turned our attention to completing the synthesis of saliniketals as shown in Scheme 10. A stereoselective reduction of aldol

Scheme 10. Completion of the Saliniketal A and B Synthesis[a]

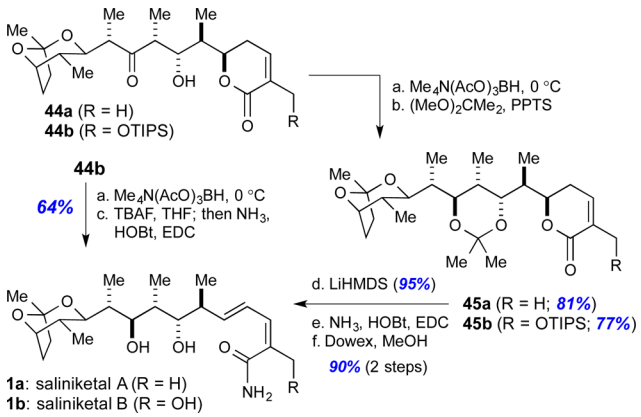

[a]Reagents and conditions: (a) $Me_4N(AcO)_3BH$, MeCN/HOAc (1:1), −20 °C; (b) $(MeO)_2CMe_2$, PPTS, acetone, rt; (c) TBAF (10 equiv), THF, rt; then NH_3(g), HOBt (2 equiv), EDC (2 equiv), rt, 72%; (d) LiHMDS (10 equiv), −78 °C, 1 h, THF, 0 °C, 95%; (e) NH_3 (1.0 M in dioxane), HOBt (2 equiv), EDC (2 equiv), THF, rt; (f) Dowex, MeOH, 1 h, rt, 90% (two steps). Abbreviations: EDC, 1-ethyl-3-(3-(dimethylamino)propyl)carbodiimide; Bt, benzotriazolyl; LiHMDS, lithium hexamethyldisilazide.

products **44a** and **44b** provided the corresponding *anti*-diols (>20:1),[30] the stereochemistry of which was confirmed via ^1H and ^{13}C NMR analysis of their acetonide derivatives **45a** and **45b**.[29] During our attempts to remove the silyl ether of the *anti*-diol derived from **44b**, we noted that tetrabutylammonium fluoride (TBAF) was basic enough to induce the subsequent dihydropyranone fragmentation.[43] This led to the development of a one-pot protocol consisting of treatment of the *anti*-diol derived from **44b** with TBAF (10 equiv) for 24 h, saturation of

DOI: 10.1021/jacs.6b03248
J. Am. Chem. Soc. 2016, 138, 7130−7142

the resulting THF solution with ammonia, and addition of the coupling reagents HOBt and EDC. After an additional 10 h of stirring at ambient temperature, saliniketal B (**1b**) was obtained in 64% overall yield for this three-step process. The spectroscopic data and optical rotation of the thus-obtained material are in full agreement with those reported by Fenical and Paterson for natural and synthetic **1b**, respectively.[5,10a]

For the synthesis of saliniketal A, we opted to explore the dihydropyranone fragmentation on acetonide **45a**, as we would need to engage a protected saliniketal A en route to the total synthesis of salinisporamycin (**2**) and rifsaliniketal (**9**) to be described later. Interestingly, the TBAF-mediated fragmentation conditions utilized for saliniketal B led to only partial conversion to the dienoic acid (~40% and 55% recovered **45a**), which led us to speculate that the corresponding fragmentation for saliniketal B was at least in part mediated by in situ-generated alkoxide (from fluoride-mediated desilylation and/or deprotonation of the C7-hydroxyl).[44] Since fluoride (TBAF) was insufficient for full conversion of **45a**, we explored other bases, among which ^{t}BuOK (THF, 0 °C, 24 h)[17a,b] and DBU (THF, rt, 48 h) also led to low conversion (13−20%, 60−65% recovered **45a**). In the end, we found a satisfactory high-yielding solution in which base-mediated fragmentation of **45a** with LiHMDS (10 equiv, THF, 0 °C) provided the desired dienoic acid in 95% yield. Amide formation as described for saliniketal B (NH_3, HOBt, EDC, THF, rt) followed by methanolysis of the acetonide protecting group yielded saliniketal A (**1a**) in 90% (two steps). Again, the spectral data were fully congruent with those reported for natural and synthetic **1a**.[5,10a] Thus, we have achieved the total synthesis of saliniketals A and B in 11−14 steps (longest linear sequence) and 27−28% overall yield from commercially available materials using two alternate but equally efficient routes to the key intermediate ethyl ketone **15**.

Salinisporamycin and Rifsaliniketal Total Synthesis: Synthesis of the Naphthoquinone and Naphthalene Fragments and Coupling with the Saliniketal A Fragment. Synthetically, we envisioned rifsaliniketal and salinisporamycin—which differ only by the presence or absence of a carboxylic acid at C4—to be derived from combining a common saliniketal A fragment with an appropriately functionalized naphthoquinone fragment via two potential routes: (1) a condensation between saliniketal acid and aminonaphthoquinone **Q** or aminonaphthalene **N** (Scheme 11, X = NH_2) or (2) transition-metal-catalyzed C−N bond formation between saliniketal A and bromonaphthoquinone **Q** or bromonaphthalene **N** (Scheme 11, X = Br).[45] Because of the prevalence of highly substituted naphthoquinones in ansamycins such as rifamycin,[46] several approaches for their synthesis have been reported.[47,48] Of those, we considered two approaches most pertinent for our goals. A Diels−Alder reaction between **46** and **47**, according to protocols explored by Trost[48c] and Roush,[48g,h] would provide facile access to bromonaphthoquinone **Q** (X = Br, R = H), whereas a cycloaddition between in situ-generated benzyne **50** (from C_2-symmetric dibromide **49**) and furan as described by Kinoshita[48e,f] would deliver oxygen-bridged cycloadduct **48**. Further elaboration of this substance would provide an alternative entry into fragments **Q**/**N** wherein R ≠ H.

The Diels−Alder approach to bromo- and aminonaphthoquinone coupling partners relevant to salinisporamycin is depicted in Scheme 12. According to a modified protocol adapted from Trost[48c] and Roush,[48g,h] Diels−Alder reaction of

Scheme 11. Strategies toward Naphthoquinone and Naphthalene Fragments for Rifsaliniketal and Salinisporamycin Total Synthesis

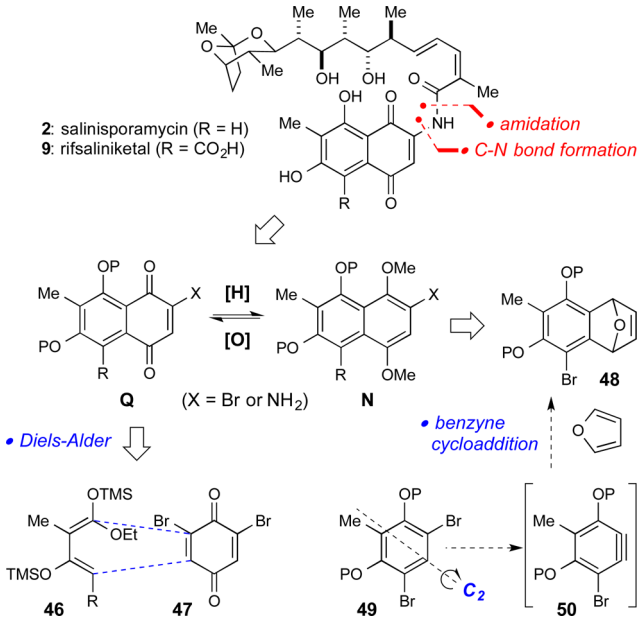

Scheme 12. Synthesis of Naphthoquinone Coupling Partners for Salinisporamycin Synthesis[a]

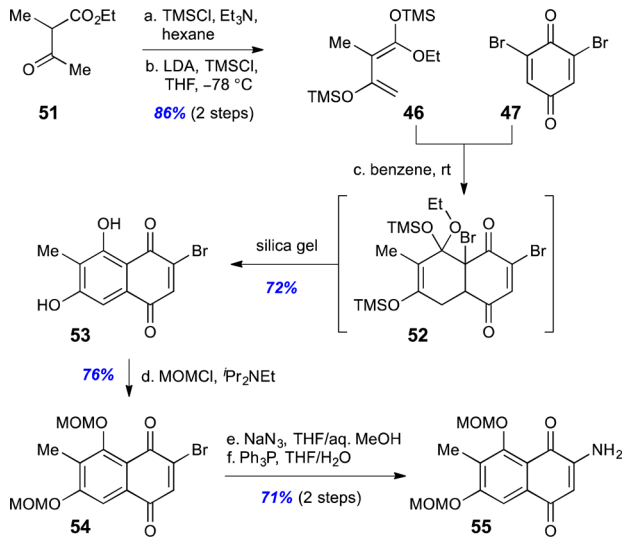

[a]Reagents and conditions: (a) Et_3N, TMSCl, hexanes, rt, 24 h; (b) ^{n}BuLi, $^i Pr_2NH$, −78 to 0 °C, then −78 °C, TMSCl, THF, 2 h, 86% (two steps); (c) benzene, rt, 6 h, then silica gel, rt, 8 h, 72%; (d) MOMCl, $^i Pr_2NEt$, CH_2Cl_2, rt, 12 h, 76%; (e) NaN_3, THF/MeOH/H_2O (9:2:2), rt, 12 h; (f) PPh_3, THF/H_2O (4:1); rt, 30 min, 71% (two steps). Abbreviation: MOM, methoxymethyl.

Brassard-like diene **46**[49] with known dibromobenzoquinone **47**[50] in benzene in the presence of silica gel afforded product **53** in 72% yield. Interestingly, when the reaction was performed in the absence of silica gel,[51] instead exploiting an aqueous HCl workup to decompose intermediate cycloadduct **52** as reported previously,[48c,g,h] no identifiable product could be isolated. Bis(methoxymethyl) protection of dihydroxynaphthoquinone **53** yielded bromonaphthoquinone coupling partner **54** in 76% yield. According to a modified protocol contributed by Boger,[52]

DOI: 10.1021/jacs.6b03248
J. Am. Chem. Soc. 2016, 138, 7130−7142

carefully controlled addition of sodium azide (the reaction is sensitive to the presence of excess azide) followed by azide reduction with triphenylphosphine in THF/H_2O afforded aminonaphthoquinone coupling partner **55** in 71% yield over two steps.

As shown in Scheme 13, reduction of bromonaphthoquinone **54** (aq. $Na_2S_2O_4$) followed by methylation of the crude reduced

Scheme 13. Synthesis of Naphthalene Coupling Partners for Salinisporamycin Synthesis[a]

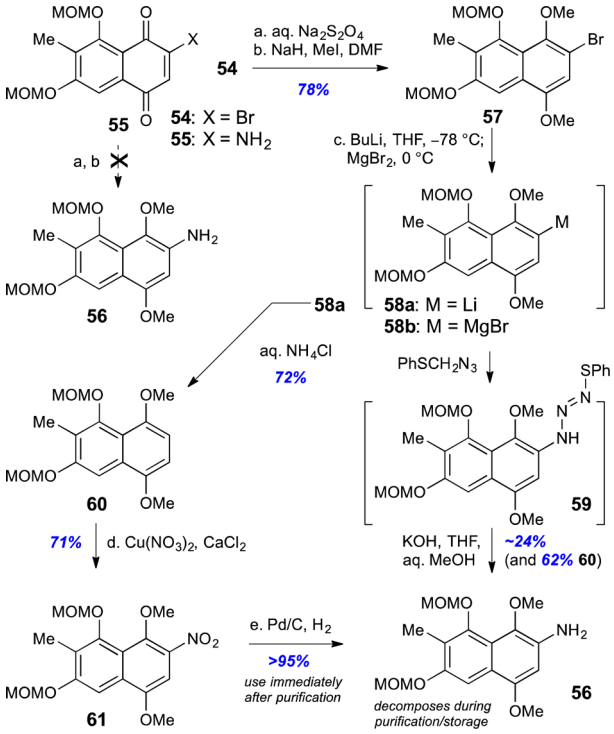

[a]Reagents and conditions: (a) $Na_2S_2O_4$, ether/H_2O (7:1), rt, 30 min; (b) NaH, MeI, DMF, rt, 12 h, 78% (two steps); (c) ^{n}BuLi, THF, −78 °C, 30 min, then $MgBr_2{\cdot}OEt_2$, 0 °C, $PhSCH_2N_3$, −78 °C, 2 h, 24% **56** (unstable) and 62% **60**; or ^{n}BuLi, THF, −78 °C, 30 min, then aq. NH_4Cl, 72% **60**; (d) $Cu(NO_3)_2{\cdot}H_2O_x$, $CaCl_2$, Ac_2O, −40 °C, 71%; (e) H_2, Pd/C, EtOAc, >95% (unstable product; used immediately in the next step).

product with MeI (NaH, DMF) afforded the more electron-rich bromonaphthalene coupling partner **57** (78% yield, two steps). Unfortunately, all attempts to reduce the corresponding aminonaphthoquinone **55** met with failure.[53] We therefore explored an amination protocol developed by Trost using azidomethylphenyl sulfide as a synthon for electrophilic NH_2^+.[48c,54] Accordingly, treatment of the Grignard derived from bromonaphthalene **57** with azidomethylphenyl sulfide followed by a basic hydrolytic workup to decompose triazene intermediate **59** provided unstable (air-sensitive) amine **56** in low yield (~24%), with the remainder of the mass balance being reduced naphthalene **60** (62%). Quenching lithium intermediate **58a** with aqueous ammonium chloride yielded **60** in 72% yield. This material proved useful for conversion to nitronaphthalene **61** using copper(II) nitrate hydrate and calcium chloride in acetic anhydride at −40 °C (71% yield).[55] Hydrogenation of **61** (Pd/C, H_2) in ethyl acetate provided target aminonaphthalene **56** in essentially quantitative yield. However, this compound proved to be very unstable and decomposed upon dissolution in chloroform or standing in air. Therefore, reduction of the stable nitro precursor **61** was best performed immediately before use.

Significant efforts—none of them successful—were devoted to the C4 functionalization of intermediates of the Diels–Alder route to salinisporamycin (Schemes 12 and 13) as an entry to coupling partners useful for rifsaliniketal synthesis (bearing an additional C4-carboxylic acid group).[56] We therefore were motivated to explore the Kinoshita benzyne cycloaddition route to naphthalenes functionalized at C4 (Scheme 14). Kinoshita

Scheme 14. Initial Benzyne Cycloaddition Route to Rifsaliniketal Naphthalene Coupling Partners[a]

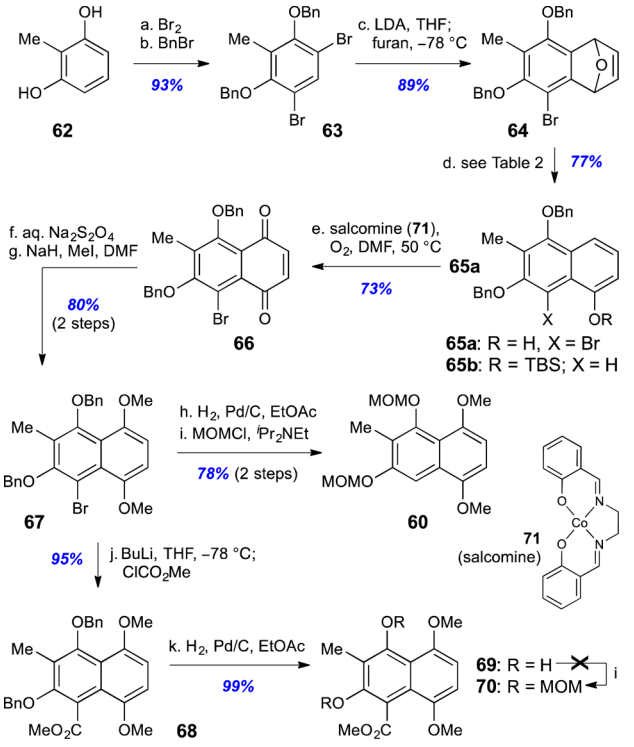

[a]Reagents and conditions: (a) Br_2, CH_2Cl_2; (b) BnBr, K_2CO_3, acetone, 93% (two steps); (c) ^{n}BuLi, $^i Pr_2NH$, −78 to 0 °C, then −78 °C, furan, warm to rt, 12 h, 89%; (d) TMSOTf, 2,6-$^t Bu_2$-pyridine, 0 °C for 5 min, then rt, 3 h, then TBAF, 0 °C, 15 min, 77%; (e) **71** (10 mol %), O_2 (1 atm), DMF, 50 °C, 12 h, 73%; (f) $Na_2S_2O_4$, ether/H_2O (3:1), 15 min, rt; (g) NaH, MeI, DMF, rt, 12 h, 80% (two steps); (h) H_2, Pd/C, EtOAc, 2 h; (i) MOMCl, $^i Pr_2NEt$, CH_2Cl_2, rt, 12 h, 78% (two steps); (j) ^{n}BuLi, $ClCO_2Me$, THF, −78 °C, 1 h, 95%; (k) H_2, Pd/C, EtOAc, 99%. Abbreviations: LDA, lithium diisopropylamide.

described the synthesis of **64** in 97% yield from the cycloaddition of furan with the benzyne generated in situ from **63** and sodium amide in THF at 57 °C.[48f] In our hands, these conditions provided **64** in unreliable yields. Instead, we found that slow addition of a solution of furan and dibromide **63** in THF over a 1 h period to a −78 °C solution of LDA in THF provided after 12 h the desired cycloadduct **64** in more reproducible yields of ~85–90%.

The subsequent ring-opening isomerization of cycloadduct **64** proved to be challenging and demanded extensive experimentation (see Table 2). Indeed, the ring-opening isomerization of a cycloadduct congener of **64** reported by Kinoshita (differing only by virtue of a C4-propanoyl substituent instead of the C4-bromide as in **64**) calls for 60%

DOI: 10.1021/jacs.6b03248
J. Am. Chem. Soc. 2016, 138, 7130–7142

Table 2. Exploration of Conditions for the Ring-Opening Isomerization of Cycloadduct 64 to Naphthol 65a[a]

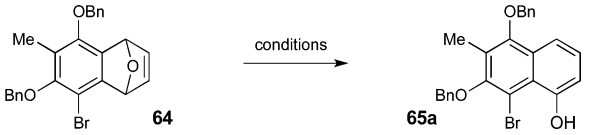

entry	conditions[b]	yield[c]
1	$HClO_4$ (5%), THF, rt, 4 h	34%
2	PPTS (20%), THF/MeOH (10:1), 40 °C, 20 h	NR
3	TsOH (5%), DCM, 40 °C, 6 h	NR
4	H_2SO_4 (5%), MeOH/H_2O (5:1), 60 °C, 6 h	NR
5	aq. HCl (12 M, 20%), MeOH, rt, 12 h	NR
6	CF_3CO_2H (5%), DCM, 40 °C, 6 h	17%
7	$Me_2C(CH_2OH)_2$, $(MeO)_3CH$, TsOH (5%), DCM, 40 °C, 12 h	23%
8	TMSI (2 equiv), DCM, 0 °C, 1 h	DC
9	TMSOTf (1 equiv), DCM, rt, 1 h	DC
10	TMSOTf (1 equiv), pyridine (1 equiv), DCM, rt, 1 h	DC
11	TMSOTf (5 equiv), 2,6-lutidine (6 equiv), THF, rt, 4 h	35%[d]
12	**TMSOTf (5 equiv), 2,6-*t*-Bu_2-pyridine (6 equiv), THF, rt, 3 h**	77%
13	TBSOTf (6 equiv), 2,6-lutidine (6 equiv), DCM, rt, 4 h	NR

[a]All reactions were performed on a 0.1 mmol scale. [b]For entries 8−13, TBAF (1 M in THF, 3 equiv) was added prior to workup to deprotect partially silylated products. [c]Isolated yields. NR = no reaction; DC = decomposition. [d]30% of the starting material was recovered.

aq. perchloric acid in THF for 35 h.[48f] These conditions completely destroyed our cycloadduct **64**. Switching to 5% aq. perchloric acid in THF provided milder conditions and partial conversion to the desired naphthol **65a** (Table 2, entry 1). Other mildly acidic conditions led to recovered starting material (entries 2−5) or low conversion (entries 6 and 7).[57] Lewis acids such as TMSI or TMSOTf (in CH_2Cl_2) were too reactive and led to decomposition (entries 8 and 9), even when buffered with pyridine (entry 10). Interestingly, the addition of 2,6-^{t}Bu$_2$-pyridine led to the desired naphthol **65a** in 77% yield (entry 12), whereas 2,6-lutidine proved to be less effective (entry 11) and the use of TBSOTf led to recovered starting material (entry 13).[58] The regiochemistry of naphthol **65a** was validated by nuclear Overhauser effect correlations obtained from derivative **65b**, congruent with results reported by Kinoshita.

Continuing with the synthesis (Scheme 14), oxidation of naphthol **65a** to quinone **66** was best performed with oxygen in the presence of the Co−salen catalyst **71** (salcomine).[59,60] Dithionite reduction of **66** followed by methylation (NaH, MeI) provided the corresponding naphthalene **67** in 80% yield (two steps). Envisioning protecting group issues later in the synthesis, we decided to switch the benzyl ether protecting groups to methoxymethyl ether protecting groups. Hydrogenolytic removal of the benzyl ethers proceeded smoothly, but the corresponding dihydroxynaphthalene **69** proved to be unstable under the conditions for methoxymethyl ether formation. We therefore decided to implement a protecting group switch earlier in the synthesis. As an aside, hydrogenation of **67** followed by MOM protection provided an alternative means of producing intermediate **60** en route to aminonaphthalene **56** (Scheme 13).

As shown in Scheme 15, transmetalation of bromide **64** (^{n}BuLi) followed by trapping with methyl chloroformate yielded methyl ester **72** in 95% yield.[48f] Ring-opening

Scheme 15. Synthesis of Rifsaliniketal Aminonaphthalene Coupling Partner 78[a]

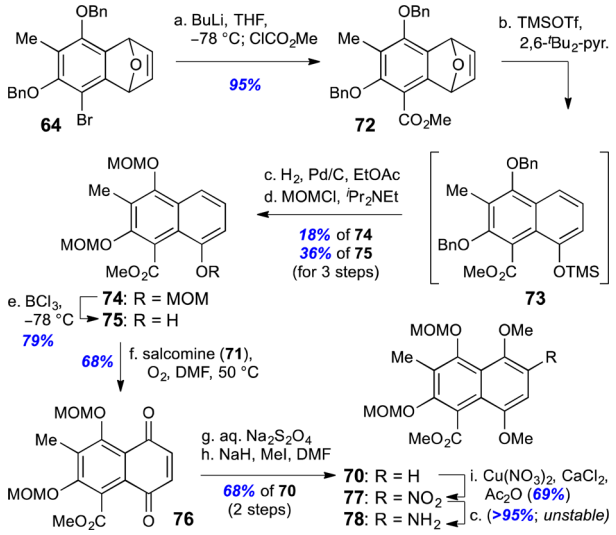

[a]Reagents and conditions: (a) ^{n}BuLi, $ClCO_2Me$, THF, −78 °C, 1 h, 95%; (b) TMSOTf, 2,6-^{t}Bu$_2$-pyridine, 0 °C for 5 min, then rt, 3 h; (c) H_2, Pd/C, EtOAc; (d) MOMCl, ^{i}Pr$_2$NEt, CH_2Cl_2, rt, 12 h, 18% **74** and 36% **75**; (e) BCl_3, −78 °C, 79%; (f) **71** (10 mol %), O_2 (1 atm), DMF, 50 °C, 12 h, 68%; (g) $Na_2S_2O_4$, ether/H_2O (5:1), rt, 15 min; (h) NaH, MeI, DMF, rt, 12 h, 68% (two steps); (i) $Cu(NO_3)_2{\cdot}H_2O_x$, $CaCl_2$, Ac_2O, −40 °C, 69%.

isomerization using the optimized conditions from Table 2, entry 12 followed by hydrogenolysis of the crude naphthol **73** then enabled installation of the methoxymethyl ether protecting groups. The desired bis(MOM ether) **75** was obtained in 36% overall yield for the three-step sequence along with tris(MOM ether) **74** (18%). The latter could be recycled to the **75** in 79% yield upon treatment with boron trichloride (for an overall yield of **75** from **72** of 52%). Salcomine-catalyzed oxidation (→ **76**, 68%),[59] dithionite reduction, and methyl ether formation proceeded smoothly as before to deliver naphthalene **70**. Nitration of **70** (using conditions optimized for nitration of **60**; Scheme 13) yielded stable nitronaphthalene **77**, which could be efficiently reduced to aminonaphthalene **78**. As before (amine **56**; Scheme 13), this substance was unstable and best prepared immediately prior to the coupling step with the saliniketal acid fragment (vide infra).

With various naphthoquinone/naphthalene fragments at hand, we explored their coupling with a suitable saliniketal surrogate (Scheme 16). Our first attempts involving a direct condensation strategy of acetonide-protected saliniketal acid **79**[61] with aminonaphthoquinone **55** invariably met with failure. A representative example includes the use of EDC and hydroxybenzotriazole (HOBt), a reagent combination that provided only the activated benzotriazolyl ester intermediate **81** (78%). Irrespective of prolonged reaction times, heating, and concentration, active ester **81** was recalcitrant to engaging the aminonaphthoquinone coupling partner **55**. Given the reduced nucleophilicity of aminonaphthoquinones,[62] we were not really surprised by these results and moved to explore a more contemporary C−N bond formation between bromonaphthoquinone **54** and protected saliniketal amide **80**.[61] However, this approach also failed, as we did not identify suitable palladium- or copper-catalyzed conditions to effect this transformation.[63−65]

DOI: 10.1021/jacs.6b03248
J. Am. Chem. Soc. 2016, 138, 7130−7142

Scheme 16. Completion of Rifsaliniketal (9) and Salinisporamycin (2) Total Synthesis[a]

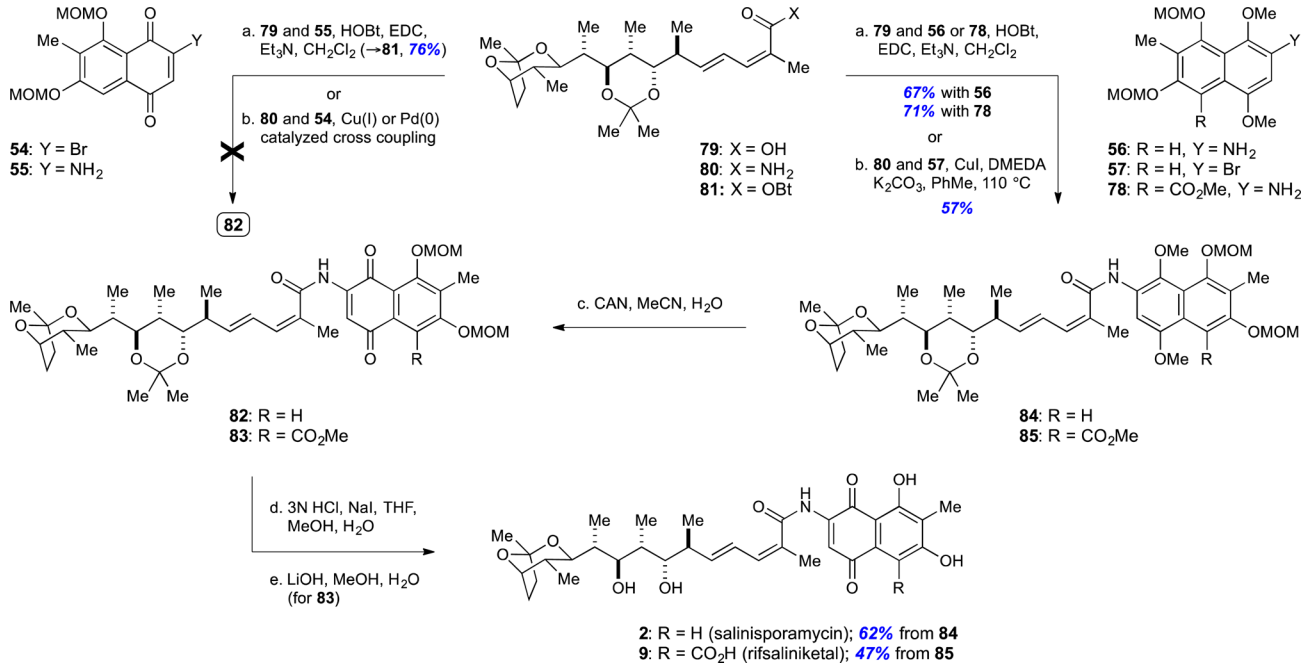

[a]Reagents and conditions: (a) **79**, **55** or **56** or **78**, HOBt, EDCI, Et_3N, CH_2Cl_2, rt, 2 h, 76% **81** (with **55**) or 67% **84** (with **56**) or 71% **85** (with **78**); (b) **80**, **57**, CuI (10 mol %), K_3PO_4, DMEDA, toluene, 100 °C, 12 h, 57%; (c) CAN, H_2O, MeCN, 0 °C, 15 min; (d) HCl, NaI, MeOH, H_2O, THF, rt, 24 h, 62% **2** (two steps from **84**); (e) crude **83**, LiOH, MeOH, H_2O, 0 °C, 12 h, 47% (three steps from **85**). Abbreviations: CAN, ceric ammonium nitrate; DMEDA, *N*,*N*′-dimethylethylenediamine.

Moving to the more electron-rich naphthalene coupling partners, we were pleased to observe a smooth Cu(I)-catalyzed cross-coupling between acetonide-protected saliniketal **80** and bromonaphthalene **57** to yield salinisporamycin precursor **84** in 57% yield according to a protocol described by Altman and Buchwald.[65d] Equally satisfying, the corresponding EDC/HOBt-mediated condensation between acetonide-protected saliniketal acid **79** and the more electron-rich aminonaphthalene **56** now also proceeded without impediment,[62] providing the same amide **84** in a slightly better isolated yield of 67%. By means of the latter procedure, rifsaliniketal amide precursor **85** was obtained in 71% yield via condensation of aminonaphthalene **78** and saliniketal acid **79**. With a viable solution at hand, the only remaining steps entailed an oxidation back to the naphthoquinoid oxidation state and global deprotection. In the event, treatment of naphthalene amides **84** and **85** with ceric ammonium nitrate in aqueous acetonitrile readily provided naphthoquinones **82** and **83**, respectively. The crude products were not purified but rather were immediately engaged in a global deprotection. Extensive experimentation was required to identify conditions for simultaneous removal of the acetonide and methoxymethyl ether protecting groups. Using substrate **82**, we found that Dowex (in MeOH) removed only the acetonide, whereas a variety of Lewis acidic conditions led to decomposition. The acetonide group was similarly removed with aqueous HCl (varying acid strength, solvents, temperature, concentration), but the phenolic methoxymethyl ethers were left largely intact. In the end, stirring an acidic solution (HCl, 0.2 N final concentration) of crude **82** and the crucial additive NaI (~1 equiv) in THF/MeOH/H_2O (10:2.5:1) for 24 h at ambient temperature cleanly delivered fully deprotected salinisporamycin (**2**) in 62% overall yield from naphthalene **84**.[66] By means of the same procedure, but with an additional saponification (aq. LiOH/MeOH), rifsaliniketal (**9**) was obtained in 47% overall yield for the three-step procedure from precursor **85**. The spectral data for synthetic **2** and **9** were in full agreement with those reported for natural **2** in ref 12 and natural **9** disclosed herein.

CONCLUSION

We have described the isolation, structure elucidation, and total synthesis of the novel marine natural product rifsaliniketal and the total synthesis of the structurally related variants salinisporamycin and saliniketals A and B. Rifsaliniketal was previously proposed, but not observed, as a diverted metabolite from a biosynthetic precursor to rifamycin S.[14] Decarboxylation of rifamycin provides salinisporamycin, which upon truncation with loss of the naphthoquinone ring leads to saliniketals. Our synthetic strategy hinged upon a Pt(II)-catalyzed cycloisomerization of an alkynediol, methodology developed in our lab,[18] to set the unique dioxabicyclo[3.2.1]octane ring system and a fragmentation of an intermediate dihydropyranone to forge a stereochemically defined (*E*,*Z*)-dienamide unit. Multiple routes were explored to assemble fragments with high stereocontrol, an exercise that provided additional insights into acyclic stereocontrol during stereochemically complex fragment-assembly processes. The resulting 11−14 step synthesis of saliniketals then enabled us to explore strategies for the synthesis and coupling of highly substituted naphthoquinones or the corresponding naphthalene fragments. A Roush/Trost Diels−Alder approach efficiently provided the heterocyclic fragments for salinisporamycin synthesis in 6−9 total steps (18−37% overall yield), whereas the corresponding carboxylic acid-containing congeners were best derived using a benzyne cycloaddition approach first explored by Kinoshita (12 total steps, 12% overall yield). Whereas direct coupling with

DOI: 10.1021/jacs.6b03248
J. Am. Chem. Soc. 2016, 138, 7130−7142

naphthoquinone fragments proved unsuccessful, both amidation and C−N bond formation tactics with the more electron-rich naphthalene congeners provided an efficient means to complete the first total synthesis of rifsaliniketal and salinisporamycin in 15−16 steps (longest linear sequence) and 13−17% overall yield from commercially available materials.

■ ASSOCIATED CONTENT

Supporting Information

The Supporting Information is available free of charge on the ACS Publications website at DOI: 10.1021/jacs.6b03248.

Rifsaliniketal isolation procedures, experimental procedures, compound characterization data, and copies of NMR spectra (PDF)

■ AUTHOR INFORMATION

Corresponding Authors

*Jef.DeBrabander@UTSouthwestern.edu

*John.MacMillan@UTSouthwestern.edu

Notes

The authors declare no competing financial interest.

■ ACKNOWLEDGMENTS

We thank Dr. Matsuda for providing NMR spectra of natural salinisporamycin and Karen MacMillan for proofreading the manuscript. Financial support was provided by the Robert A. Welch Foundation (Grants I-1422 and I-1689). J.K.D. holds the Julie and Louis Beecherl, Jr., Chair in Medical Science, and J.B.M. is a Chilton/Bell Scholar in Biochemistry.

■ REFERENCES

(1) Prudhomme, J.; McDaniel, E.; Ponts, N.; Bertani, S.; Fenical, W.; Jensen, P.; Le Roch, K. *PLoS One* **2008**, *3*, e2335.

(2) Jensen, P. R.; Mafnas, C. *Environ. Microbiol.* **2006**, *8*, 1881−1888.

(3) Feling, R. H.; Buchanan, G. O.; Mincer, T. J.; Kauffman, C. A.; Jensen, P. R.; Fenical, W. *Angew. Chem., Int. Ed.* **2003**, *42*, 355−357.

(4) Udwary, D. W.; Zeigler, L.; Asolkar, R. N.; Singan, V.; Lapidus, A.; Fenical, W.; Jensen, P. R.; Moore, B. S. *Proc. Natl. Acad. Sci. U. S. A.* **2007**, *104*, 10376−10381.

(5) Williams, P. G.; Asolkar, R. N.; Kondratyuk, T.; Pezzuto, J. M.; Jensen, P. R.; Fenical, W. *J. Nat. Prod.* **2007**, *70*, 83−88.

(6) Gerner, E. W.; Meyskens, F. L., Jr. *Nat. Rev. Cancer* **2004**, *4*, 781−792.

(7) Pendeville, H.; Carpino, N.; Marine, J. C.; Takahashi, Y.; Muller, M.; Martial, J. A.; Cleveland, J. L. *Mol. Cell. Biol.* **2001**, *21*, 6549−6558.

(8) Saunders, L. R.; Verdin, E. *Mol. Cancer Ther.* **2006**, *5*, 2777−2785.

(9) Basuroy, U. K.; Gerner, E. W. *J. Biochem.* **2006**, *139*, 27−33.

(10) For total syntheses, see: (a) Paterson, I.; Razzak, M.; Anderson, E. A. *Org. Lett.* **2008**, *10*, 3295−3298. (b) Liu, J.; De Brabander, J. K. *J. Am. Chem. Soc.* **2009**, *131*, 12562−12563.

(11) For a formal synthesis, see: Yadav, J. S.; Hossain, S. S.; Madhu, M.; Mohapatra, D. K. *J. Org. Chem.* **2009**, *74*, 8822−8825.

(12) Matsuda, S.; Adachi, K.; Matsuo, Y.; Nukina, M.; Shizuri, Y. *J. Antibiot.* **2009**, *62*, 519−526.

(13) (a) Jensen, P. R.; Williams, P. G.; Oh, D.-C.; Zeigler, L.; Fenical, W. *Appl. Environ. Microbiol.* **2007**, *73*, 1146−1152. (b) Kim, T. K.; Hewavitharana, A. K.; Shaw, P. N.; Fuerst, J. A. *Appl. Environ. Microbiol.* **2006**, *72*, 2118−2125. (c) Bose, U.; Hewavitharana, A. K.; Vidgen, M. E.; Ng, Y. K.; Shaw, P. N.; Fuerst, J. A.; Hodson, M. P. *PLoS One* **2014**, *9*, e91488.

(14) Wilson, M. C.; Gulder, T. A.; Mahmud, T.; Moore, B. S. *J. Am. Chem. Soc.* **2010**, *132*, 12757−12765.

(15) Espindola, A. P.; Crouch, R.; DeBergh, J. R.; Ready, J. M.; MacMillan, J. B. *J. Am. Chem. Soc.* **2009**, *131*, 15994−15995.

(16) See Table S2 in the Supporting Information for a comparison of the ^{1}H and ^{13}C NMR data of salinisporamycin and rifsaliniketal.

(17) This interesting fragmentation is rarely used in total synthesis. For selected examples, see: (a) Corey, E. J.; Schmidt, G. *Tetrahedron Lett.* **1979**, *20*, 2317−2320. (b) Roush, W. R.; Spada, A. P. *Tetrahedron Lett.* **1982**, *23*, 3773−3776. (c) Masamune, S.; Imperiali, B.; Garvey, D. S. *J. Am. Chem. Soc.* **1982**, *104*, 5528−5531.

(18) Liu, B.; De Brabander, J. K. *Org. Lett.* **2006**, *8*, 4907−4910.

(19) For a related bidirectional approach in the context of rifamycin, see ref 17c.

(20) For selected reviews, see: (a) Roush, W. *J. Org. Chem.* **1991**, *56*, 4151−4157. (b) Franklin, A. S.; Paterson, I. *Contemp. Org. Synth.* **1994**, *1*, 317−338. For a computational study, see: (c) Gennari, C.; Vieth, S.; Comotti, A.; Vulpetti, A.; Goodman, J. M.; Paterson, I. *Tetrahedron* **1992**, *48*, 4439−4458.

(21) For selected examples, see: (a) Martin, S. F.; Lee, W.-C. *Tetrahedron Lett.* **1993**, *34*, 2711−2714. (b) Evans, D. A.; Dart, M. J.; Duffy, J. L.; Rieger, D. L. *J. Am. Chem. Soc.* **1995**, *117*, 9073−9074. (c) Evans, D. A.; Yang, M. G.; Dart, M. J.; Duffy, J. L. *Tetrahedron Lett.* **1996**, *37*, 1957−1960.

(22) Dess, D. B.; Martin, J. C. *J. Org. Chem.* **1983**, *48*, 4155−4156.

(23) Brown, H. C.; Bhat, K. S. *J. Am. Chem. Soc.* **1986**, *108*, 5919−5923.

(24) ^{1}H NMR analysis of the crude mixture indicated the presence of all four possible diastereomers in addition to the starting material and unidentified material.

(25) The stereochemistry of the aldol product **18**-*syn* was assigned by comparison to the same ethyl ketone product obtained from **21**-*syn* via treatment of **21**-*syn* with ethylmagnesium bromide (CH_2Cl_2, −78 °C, 33% yield). See the Supporting Information for details.

(26) Increasing the reaction time and/or the temperature (to −50 °C) led to the formation of significant amounts of desilylated, dehydrated cyclic dienol ether byproduct **19**. See the Supporting Information for details.

(27) Unlike other *syn*-α-Me,β-alkoxyaldehydes, aldehyde **13** contains a terminal alkyne, which might be responsible for the observed Felkin aldol selectivity. In this context, we note that Danishefsky and coworkers have observed an effect of π-electron substituents (olefin, aryl) on aldehyde facial bias through long-range nonbonding interactions between the aldehyde and substituent π systems. See: Lee, C. B.; Wu, Z.; Zhang, F.; Chappell, M. D.; Stachel, S. J.; Chou, T.-C.; Guan, Y.; Danishefsky, S. J. *J. Am. Chem. Soc.* **2001**, *123*, 5249−5259.

(28) Crimmins, M. T.; King, B. W.; Tabet, E. A.; Chaudhary, K. *J. Org. Chem.* **2001**, *66*, 894−902.

(29) (a) Rychnovsky, S. D.; Skalitzky, D. J. *Tetrahedron Lett.* **1990**, *31*, 945−948. (b) Evans, D. A.; Rieger, D. L.; Gage, J. R. *Tetrahedron Lett.* **1990**, *31*, 7099−7100.

(30) Evans, D. A.; Chapman, K. T.; Carreira, E. M. *J. Am. Chem. Soc.* **1988**, *110*, 3560−3578.

(31) (a) Evans, D. A.; Clark, J. S.; Metternich, R.; Novack, V. J.; Sheppard, G. S. *J. Am. Chem. Soc.* **1990**, *112*, 866−868. (b) Evans, D. A.; Ng, H. P.; Clark, S.; Rieger, D. L. *Tetrahedron* **1992**, *48*, 2127−2142.

(32) The **22**-*anti* diol thus prepared was identical to that prepared according to Scheme 4. The structures of **27** and **22**-*anti* were confirmed after transformation to the same primary alcohol obtained from hydrogenolysis of **32** or $LiBH_4$ reduction of **33** and comparison to the same alcohol prepared independently by Paterson et al.[10a] See the Supporting Information.

(33) Nicolaou, K. C.; Patron, A. P.; Ajito, K.; Richter, P. K.; Khatuya, H.; Bertinato, P.; Miller, R. A.; Tomaszewski, M. J. *Chem. - Eur. J.* **1996**, *2*, 847−868.

(34) It should be noted that the stereochemical outcome is not important, as the resulting stereocenter will be destroyed during the final dihydropyranone fragmentation reaction (Scheme 10). However, homogeneous material facilitates characterization, and targeting the

DOI: 10.1021/jacs.6b03248
J. Am. Chem. Soc. 2016, 138, 7130−7142

syn stereoisomer was predicted to provide maximal stereocontrol during the aldol fragment coupling in this double diastereodifferentiating process.

(35) Yu, C.; Liu, B.; Hu, L. *J. Org. Chem.* **2001**, *66*, 5413−5418.

(36) Scholl, M.; Ding, S.; Lee, C. W.; Grubbs, R. H. *Org. Lett.* **1999**, *1*, 953−956.

(37) (a) Gustin, D. J.; VanNieuwenhze, M. S.; Roush, W. R. *Tetrahedron Lett.* **1995**, *36*, 3447−3450. (b) McCarthy, P. A.; Kageyama, M. *J. Org. Chem.* **1987**, *52*, 4681−4686. (c) Paterson, I.; McClure, C. K. *Tetrahedron Lett.* **1987**, *28*, 1229−1232. (d) Duffy, J. L.; Yoon, T. P.; Evans, D. A. *Tetrahedron Lett.* **1995**, *36*, 9245−9248.

(38) The selectivity tends to be largely independent of the nature and relative configuration of the enolate β-alkoxy substituent.

(39) For a review of allylic 1,3-strain, see: Hoffmann, R. W. *Chem. Rev.* **1989**, *89*, 1841−1860.

(40) For an insightful analysis, see ref 37a.

(41) This particular stereochemical combination of lithium enolate and aldehyde was classified as a fully mismatched case.[20c] Similar literature examples of fully mismatched reactions provided aldol products in a nonselective manner.[21a,c,37a]

(42) Because lithium enolates are typically not monomeric, a chelated transition state akin to **II** (Figure 2) could engage the aldehyde via a second distinct lithium atom. To avoid developing *syn*-pentane interactions with the ethylene bridge (as in **TTS-chelate**), it would be anticipated that the aldehyde would engage the less-hindered enolate *Si* face in such a situation.

(43) Nakata, T.; Hata, N.; Oishi, T. *Heterocycles* **1990**, *30*, 333−334.

(44) TBAF can contain significant amounts of hydroxide, which is potentially the base in the reaction. The poor reactivity could be due to the need for a primary hydroxymethyl and/or C7-hydroxyl to act as an internal base, both of which are absent in acetonide **45a**.

(45) Given a potential facile redox interconversion, we envisioned that both naphthoquinone **Q** and naphthalene **N** intermediates would be viable coupling partners.

(46) Floss, H. G.; Yu, T.-W. *Chem. Rev.* **2005**, *105*, 621−632.

(47) For selected total syntheses, see: (a) Rifamycin S: Kishi, Y. *Pure Appl. Chem.* **1981**, *53*, 1163−1180. (b) Rifamycin W: Nakata, M.; Akiyama, N.; Kamata, J.-i.; Kojima, K.; Masuda, H.; Kinoshita, M.; Tatsuta, K. *Tetrahedron* **1990**, *46*, 4629−4652. (c) Damavaricin D: Roush, W. R.; Coffey, D. S.; Madar, D. J. *J. Am. Chem. Soc.* **1997**, *119*, 11331−11332.

(48) For selected approaches relevant to the work described here, see: (a) Kozikowski, A. P.; Sugiyama, K.; Springer, J. P. *Tetrahedron Lett.* **1980**, *21*, 3257−3260. (b) Parker, K. A.; Petraitis, J. J. *Tetrahedron Lett.* **1981**, *22*, 397−400. (c) Trost, B. M.; Pearson, W. H. *Tetrahedron Lett.* **1983**, *24*, 269−272. (d) Kelly, R. T.; Behforouz, M.; Echavarren, A.; Vaya, J. *Tetrahedron Lett.* **1983**, *24*, 2331−2334. (e) Nakata, M.; Kinoshita, M.; Ohba, S.; Saito, Y. *Tetrahedron Lett.* **1984**, *25*, 1373−1376. (f) Nakata, M.; Wada, S.; Tatsuta, K.; Kinoshita, M. *Bull. Chem. Soc. Jpn.* **1985**, *58*, 1801−1806. (g) Roush, W. R.; Madar, D. J. *Tetrahedron Lett.* **1993**, *34*, 1553−1556. (h) Roush, W. R.; Coffey, D. S. *J. Org. Chem.* **1995**, *60*, 4412−4418. (i) Kuttruff, C. A.; Geiger, S.; Cakmak, M.; Mayer, P.; Trauner, D. *Org. Lett.* **2012**, *14*, 1070−1073. (j) Nawrat, C. C.; Palmer, L. I.; Blake, A. J.; Moody, C. J. *J. Org. Chem.* **2013**, *78*, 5587−5603. (k) Nawrat, C. C.; Lewis, W.; Moody, C. J. *J. Org. Chem.* **2011**, *76*, 7872−7881.

(49) Langer, P.; Schneider, T.; Stoll, M. *Chem. - Eur. J.* **2000**, *6*, 3204−3214.

(50) For the preparation of **47**, see: Bringmann, G.; Götz, R.; Keller, P. A.; Walter, R.; Boyd, M. R.; Lang, F.; Garcia, A.; Walsh, J. J.; Tellitu, I.; Bhaskar, K. V.; Kelly, T. R. *J. Org. Chem.* **1998**, *63*, 1090−1097.

(51) For a similar beneficial effect of silica gel on aromatization of Diels−Alder intermediates en route to naphthomycin, see ref 48i.

(52) Boger, D. L.; Panek, J. S.; Duff, S. R.; Yasuda, M. *J. Org. Chem.* **1985**, *50*, 5790−5795.

(53) In addition to dithionite reduction, Luche reduction (see: Gemal, A. L.; Luche, J. L. *J. Am. Chem. Soc.* **1981**, *103*, 5454−5459) and various hydrogenation conditions were explored..

(54) Trost, B. M.; Runge, T. A. *J. Am. Chem. Soc.* **1981**, *103*, 2485−2487.

(55) The conditions reported by Kinoshita failed, which we attributed to the presence of crystal water in commercially available $Cu(NO_3)_2$. The addition of dry $CaCl_2$ provided an efficient solution. See: Gandy, M. N.; Piggott, M. J. *J. Nat. Prod.* **2008**, *71*, 866−868.

(56) We explored various Friedel−Crafts acylation conditions and halogenations with intermediates from Schemes 12 and 13 as well as congeners with various alternative protecting groups instead of MOM.[48g] Attempts to access more elaborate dienes for early C4 introduction during the Diels−Alder reaction were equally frustrating. See, for example, ref 48d,j and: Okabayashi, T.; Iida, A.; Takai, K.; Nawate, Y.; Misaki, T.; Tanabe, Y. *J. Org. Chem.* **2007**, *72*, 8142−8145.

(57) (a) Sörgel, S.; Azap, C.; Reißig, H.-U. *Eur. J. Org. Chem.* **2006**, *2006*, 4405−4418. (b) Blanchot, M.; Candito, D. A.; Larnaud, F.; Lautens, M. *Org. Lett.* **2011**, *13*, 1486−1489. (c) Kaelin, D. E.; Lopez, O. D.; Martin, S. F. *J. Am. Chem. Soc.* **2001**, *123*, 6937−6938. (d) Batt, D.; Jones, D. G.; La Greca, S. *J. Org. Chem.* **1991**, *56*, 6704−6708. (e) Morton, G. E.; Barrett, A. G. M. *J. Org. Chem.* **2005**, *70*, 3525−3529. (f) Etomi, N.; Kumamoto, T.; Nakanishi, W.; Ishikawa, T. *Beilstein J. Org. Chem.* **2008**, *4*, 15.

(58) Magnus, P.; Eisenbeis, S. A.; Fairhurst, R. A.; Iliadis, T.; Magnus, N. A.; Parry, D. *J. Am. Chem. Soc.* **1997**, *119*, 5591−5605.

(59) De Jonge, C. R. H. I.; Hageman, H. J.; Hoentjen, G.; Mijs, W. *Org. Synth.* **1977**, *57*, 78.

(60) Oxidation with $PhI(OAc)_2$, Ag_2O (dioxane/HNO_3), NBS ($HOAc/H_2O$), or iron(III) salts did not produce the desired 1,4-naphthoquinone. See ref 58 and: (a) Kitani, Y.; Morita, A.; Kumamoto, T.; Ishikawa, T. *Helv. Chim. Acta* **2002**, *85*, 1186−1195. (b) Möller, K.; Wienhöfer, G.; Schröder, K.; Join, B.; Junge, K.; Beller, M. *Chem. - Eur. J.* **2010**, *16*, 10300−10303.

(61) Acetonide-protected acid **79** and amide **80** are intermediates en route to saliniketal A. See the Supporting Information.

(62) For similar observations regarding a recalcitrant intramolecular macrolactamization of a rifamycin-derived aminoquinoid carboxylic acid and a solution via the use of the more electron-rich aminodihydroquinoid carboxylic acid, see: Corey, E. J.; Clark, D. A. *Tetrahedron Lett.* **1980**, *21*, 2045−2048.

(63) To the best of our knowledge, there are no reported examples of amidation of halo-substituted naphthoquinones similar to bromide **55** via C−N bond formation.

(64) For a user's guide to palladium-catalyzed aminations and amidations, see: Surry, D. S.; Buchwald, S. L. *Chem. Sci.* **2011**, *2*, 27−50.

(65) For a review, see: (a) Surry, D. S.; Buchwald, S. L. *Chem. Sci.* **2010**, *1*, 13−31. For selected examples, see: (b) Klapars, A.; Huang, X.; Buchwald, S. L. *J. Am. Chem. Soc.* **2002**, *124*, 7421−7428. (c) Jiang, L.; Job, G. E.; Klapars, A.; Buchwald, S. L. *Org. Lett.* **2003**, *5*, 3667−3669. (d) Altman, R. A.; Buchwald, S. L. *Nat. Protoc.* **2007**, *2*, 2474−2479.

(66) For an example of the beneficial use of NaI as an additive during methoxymethyl ether deprotection, see: Williams, D. R.; Barner, B. A.; Nishitani, K.; Phillips, J. G. *J. Am. Chem. Soc.* **1982**, *104*, 4708−4710.

DOI: 10.1021/jacs.6b03248
J. Am. Chem. Soc. 2016, 138, 7130−7142